Biophysical Journal
Biophysical Perspective

Biophysical Society

Voltage and Calcium Imaging of Brain Activity

Masoud Sepehri Rad,[1,*] Yunsook Choi,[2,3] Lawrence B. Cohen,[1,2,3,*] Bradley J. Baker,[1,*] Sheng Zhong,[2] Douglas A. Storace,[2,3] and Oliver R. Braubach[1,3]

[1]Center for Functional Connectomics, Korea Institute of Science and Technology, Seoul, Republic of Korea; [2]Department of Cellular and Molecular Physiology, Yale University School of Medicine, New Haven, Connecticut; and [3]NeuroImaging Cluster, Marine Biological Laboratory, Woods Hole, Massachusetts

ABSTRACT Sensors for imaging brain activity have been under development for almost 50 years. The development of some of these tools is relatively mature, whereas qualitative improvements of others are needed and are actively pursued. In particular, genetically encoded voltage indicators are just now starting to be used to answer neurobiological questions and, at the same time, more than 10 laboratories are working to improve them. In this Biophysical Perspective, we attempt to discuss the present state of the art and indicate areas of active development.

Optical measurements of brain activity are attractive because they allow for simultaneous and noninvasive monitoring of activity from many individual neurons or from many different brain regions (population signals). In 1937, Sherrington imagined points of light signaling the activity of nerve cells and their connections. During sleep, only a few remote parts of the brain would twinkle, but, at awakening, "Swiftly the head-mass becomes an enchanted loom where millions of flashing shuttles weave a dissolving pattern" (1). In the 80 years since, there has been significant progress: optical measurements of neural activity are now a reality. This perspective is restricted to imaging activity in mammalian preparations. For earlier reviews and perspectives, see (2–5).

A large parameter space for imaging activity

Different preparations. Even considering only mammalian preparations, the variations in imaging possibilities and scientific goals are large. Neurons in culture can be studied with wide-field optics and very intense illumination. Brain slice and in vivo preparations are both strongly scattering and, except for cells and processes that are very close to the surface or in situations of very sparse genetically encoded voltage indicator (GEVI) expression, single cell resolution requires two-photon microscopy. Illumination intensities for in vivo measurements are limited by the damage that results from high intensities. Podgorski and Ranganathan (6) found that continuous illumination of a 1 mm^2 area produced a temperature increase of 1.8°C/100 mW.

Different measurement goals: individual neurons and population signals. For some scientific aims, single cell resolution of activity is important. For others, population signals are preferable. For example, the input to each glomerulus in the olfactory bulb is carried by >1000 axons from receptor cells in the nose. Measuring the activity from individual receptor nerve terminals is not presently feasible and might not be that informative. However, measuring the population average of the input to the glomerulus was possible (7,8), and has proven to be useful in studying olfactory bulb function (e.g., (8–10)).

Different sensors: organic dyes and genetically encoded voltage and calcium sensors. The development of organic voltage- and calcium-sensitive dyes started in the 1970s (11–13). Presently available organic voltage-sensitive dyes are very fast ($\tau \sim <<1$ ms) and have large signals (>50%/100 mv). They remain the sensors of choice in some measurements; for example, recording activity in individual dendrites and spines in in vitro preparations (e.g., (14,15)). Those measurements were made after injecting the dye into an individual neuron, thereby eliminating interference from fluorescence of surrounding cells and processes. In addition, organic calcium-sensitive dyes often remain the sensors of choice for in vivo two-photon measurements of individual neuron activity. However, an important limitation of organic dyes is the absence of cell-type specificity. Bathing an in vitro or an in vivo preparation with an organic voltage-sensitive dye will stain the external membranes of all of the neurons, the glia, and the

Submitted June 8, 2017, and accepted for publication September 21, 2017.

*Correspondence: masoud.sepehri15@yahoo.com or lawrence.b.cohen@hotmail.edu or bradley.baker19@gmail.com

Editor: Brian Salzberg.

https://doi.org/10.1016/j.bpj.2017.09.040

vasculature. Disambiguating the source of the signal in these measurements is difficult. In contrast, there are many mammalian transgenic animals with cre recombinase expressed in individual cell types. This has been accompanied by the development of GEVIs and genetically encoded calcium indicators (GECIs) that can take advantage of these transgenic animals and provide individual cell type specificity in the measurement of brain activity.

Three types of GEVIs

The first GEVI developed in a laboratory was a mosaic constructed by inserting a fluorescent protein (FP) into a voltage-sensitive protein that resided in the plasma membrane. The sensor, FlaSh (16), was a voltage-gated potassium channel with GFP inserted after the sixth transmembrane segment. Aside from its importance as a proof of principle, FlaSh had the useful feature of a steep, sigmoidal fluorescence-versus-voltage relationship that could be tuned to select for different ranges of membrane potential. However, FlaSh also had drawbacks; its signal was relatively slow ($\tau \sim 100$ ms), and small ($\Delta F/F < 5\%$). But, most importantly, FlaSh, and the analog Flare (17), worked in frog oocytes but not at all in mammalian cells. In mammalian cells, Flare's expression was mainly intracellular (18). This obstacle was overcome by the Knöpfel laboratory, who changed the membrane resident voltage sensor to the voltage-sensitive domain of the *Ciona intestinalis* voltage-sensitive phosphatase (19).

Comparison of GEVI structures

Mosaic GEVIs. A number of recent GEVI developments have focused on mosaic proteins using the voltage-sensitive domain of the *Ciona* voltage-sensitive phosphatase as well as analogs from other vertebrate species. Three varieties of mosaic GEVIs are illustrated schematically in Fig. 1 *A*. The left panel illustrates a single FP mosaic (e.g., ArcLight (20)); the middle panel shows a mosaic with a "butterfly" fluorescence resonance energy transfer (FRET) pair of fluorescent proteins, where the two FPs are on opposite sides of the voltage-sensitive domain (e.g., VSFP-Butterfly 1.2 (21)); and the right panel is a mosaic with a circularly permuted fluorescent protein inserted in the external loop between transmembrane segments 3 and 4 (e.g., ASAP1 (22)).

Bacterial rhodopsin-based GEVIs. A second type of GEVI utilizes the voltage sensitivity of microbial rhodopsins (Fig. 1 *B* (23)). Both the absorption and fluorescence of the microbial rhodopsins are voltage sensitive but their fluorescence quantum efficiency is ~100 times smaller than GFP and thus single chromophore type 2 GEVIs (*left panel*) require high intensity illumination to achieve an adequate signal-to-noise ratio (e.g., Arch (24)). With

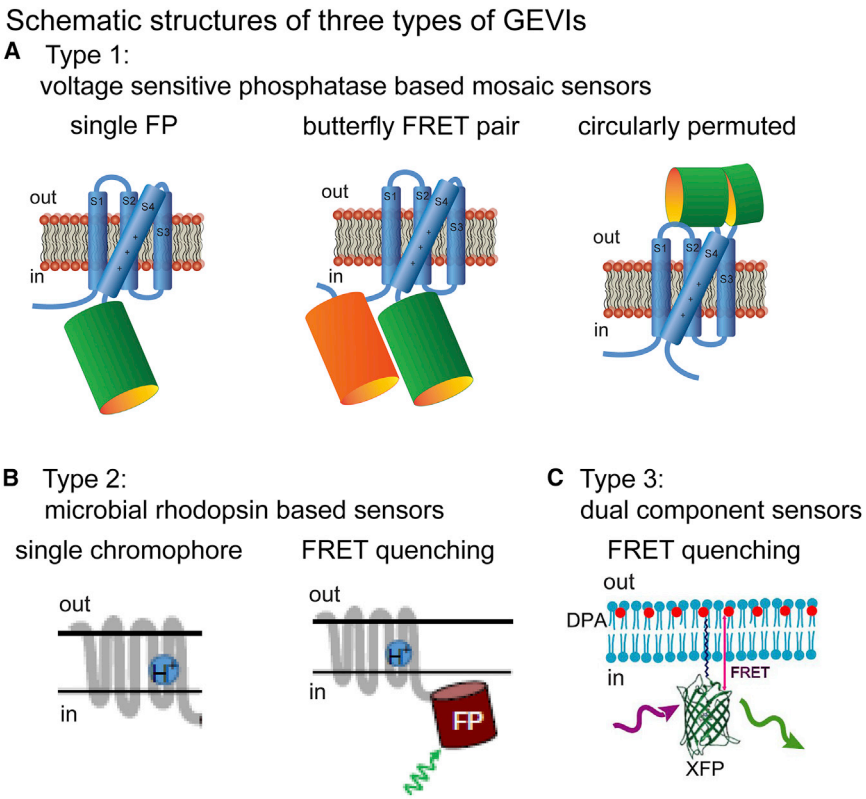

FIGURE 1 Schematic structures of three types of GEVIs. (*A*) Given here are mosaic sensors combining the voltage-sensitive domain of a voltage-sensitive phosphatase and a fluorescent protein. (*B*) Given here are sensors based on the voltage sensitivity of a microbial rhodopsin. (*C*) Given here are sensors that are a combination of two separate molecules. (*B*) Modified from (61). (*C*) Modified from (32).

in vivo mammalian CNS preparations, these illumination intensities are expected to be damaging. By combining the microbial rhodopsin in a mosaic with a second, bright, fluorescent protein (Fig. 1 *B*, *right panel*), a voltage-sensitive FRET quenching signal is obtained (e.g., Ace2N-4AA)-mNeon (25)).

Two-component GEVIs. A third type of GEVI is a two-component sensor that utilizes FRET quenching between a membrane-bound fluorescent protein and a mobile charged membrane resident molecule as the voltage sensor (Fig. 1 *C*; e.g., hVOS (26)). The voltage sensor, dipicrylamine, in hVOS must be externally applied by the experimenter.

Voltage versus calcium indicators

Beginning in 2003 (27), calcium signals have been used as surrogates for a direct measure of action potentials in single cell measurements based on the assumptions that action potentials are the only source of the measured calcium changes and that calcium changes occur during action potentials in all types of neurons. These assumptions are certainly not universally true (28,29). For example, subthreshold depolarizations elicited clear calcium transients in mitral cells (28). Calcium influx can also occur through ligand-gated receptors (30,31) and can be further modulated by release from internal stores of calcium (32–34). In addition, the fact that voltage-gated calcium channels only open at a certain membrane potential creates a threshold effect. Also, many GECIs have further nonlinearities resulting from Hill coefficients that are as great as three (35). Calcium dynamics are also slow in contrast to voltage changes; this blurs the relationship between the optical signal and spike rates except at very low rates (36–38). Optical measurements from GECIs can be further confounded by the kinetics of the protein sensor (39,40). Finally, hyperpolarizations are likely to be missed by GECIs whereas the mosaic sensor GEVIs (Fig. 1 *A*) can be tuned to respond differentially to hyperpolarization or depolarization (41,42). Nonetheless, a combination of the large signal-to-noise ratios of GECIs and, until recently, the quite small signal-to-noise ratios of GEVIs led to the nearly universal use of GECIs. An additional advantage for GEVIs is that the calcium changes and the resulting signals are much slower and thus are better suited to the frame rates available in two-photon imaging. Recent reviews of calcium imaging and GECIs are available elsewhere (31,35,43).

With the development of GEVIs with improved signal-to-noise ratios and faster response times, GEVI measurements of activity are starting to be used to answer neurobiological questions (e.g., (9,25,44–46)). Future GEVI improvements would increase the range of experiments where GEVIs can make an important contribution.

Comparison of GEVIs and GECIs in mammalian preparations

Population signals. Fig. 2 *A* illustrates six repeated measurements of the in vivo response to ethyl tiglate from a single glomerulus in a preparation where the mitral/tufted cells and their dendritic tufts in the glomerulus expressed the GEVI ArcLight (20). The repeated trials overlap; thus, over this timescale, phototoxicity was minimal. Fig. 2 *B* shows paired recordings of ArcLight and GCaMP3 (Fig. 2 *B1*) and ArcLight and GCaMP6f (Fig. 2 *B2*) in opposite hemibulbs in response to two inspirations of ethyl tiglate. The odor presentations resulted in breath-coupled responses that were obvious with ArcLight, but can only be discerned with difficulty using GCaMP3 and were relatively small with GCaMP6f. On the other hand, ArcLight had a smaller $\Delta F/F$ and signal-to-noise ratio than the GCaMPs (40). Carandini et al. (47) compared GEVI signals (VSFP-Butterfly 1.2) and GECI signals (GCaMP3) in visual cortex. In some circumstances (brief stimuli), the GECI had a larger signal-to-noise ratio, whereas for

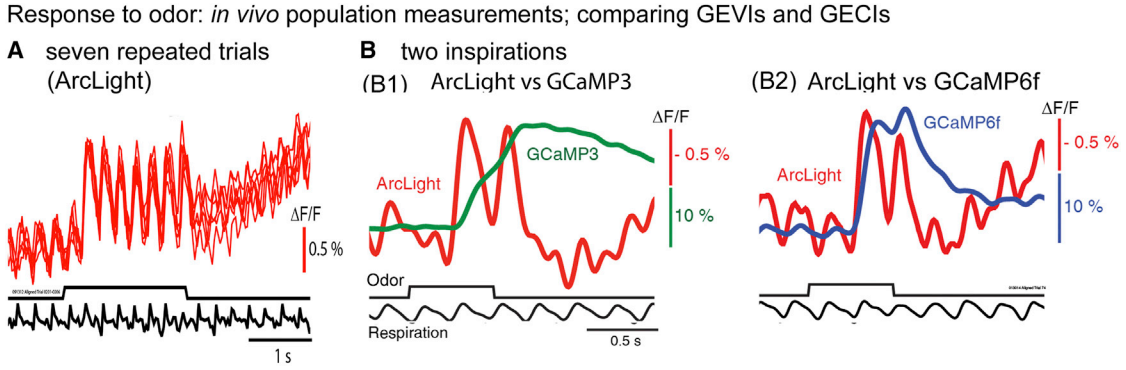

FIGURE 2 In vivo population measurements. Comparing GEVIs and GECIs. (*A*) Shown here are in vivo population measurements using ArcLight, a single FP mosaic GEVI. The mitral-tufted cells were transduced by infection with an AAV1 virus containing ArcLight DNA. An overlay of the responses to six repeated trials from a single glomerulus to the odorant ethyl tiglate presented during seven breaths. There was little change from trial to trial. (*B*) Given here is a comparison of ArcLight and GCaMP3 (*B1*) or GCaMP6f (*B2*) signals from opposite olfactory bulbs in the same preparations over response to odorant presentations lasting two breaths. The ArcLight responses are faster. Modified from (12).

steady-state stimuli the GECI and GEVI signal-to-noise ratios were similar.

Single cell signals. ArcLight, the GEVI used In Fig. 2, responds to a step change in membrane potential with two time constants; the fast one is ~10 ms. Thus, the response to a neuronal action potential (~3%) is much smaller than the response to a long voltage step in HEK293 cells (~40%). A faster GEVI would be more efficient. Fig. 3 (22) shows that a much faster GEVI, ASAP1 ($\tau \sim 2$ ms), can follow individual spike potential changes with good temporal resolution. ASAP1 and other faster GEVIs can provide precise spike timing at spike rates much higher than is possible using GECIs.

ArcLight's ability to report odor-evoked activity in single trials and Ace2N-4AA-mNeon ability to follow individual spikes in individual cortical neurons shows that GEVIs could be a useful tool for in vivo measurements (see below). That said, GEVIs and GECIs are complementary tools, where the appropriate choice depends on whether the improved temporal resolution and membrane potential sensitivity of GEVIs is more important than the better signal-to-noise ratio and calcium sensitivity of the GCaMPs.

GEVI sensor choice

Population recordings. In population recordings, a large signal is likely to be more important than a fast response. In that situation, ArcLight, a relatively bright sensor with a relatively large $\Delta F/F$ and signal-to-noise ratio, would be a good choice. ArcLight AAV virus preparations are available from the Penn Vector Core (https://pennvectorcore.med.upenn.edu/).

Single cell recordings. Here a relatively bright GEVI with a fast response ($\tau \sim 1$ ms) is important. FlicR1 ((48), Ace2N-mNeon (25), ASAP1 (22), or Bongwoori-R3 (49)) had good signal-to-noise ratios in cultured neurons.

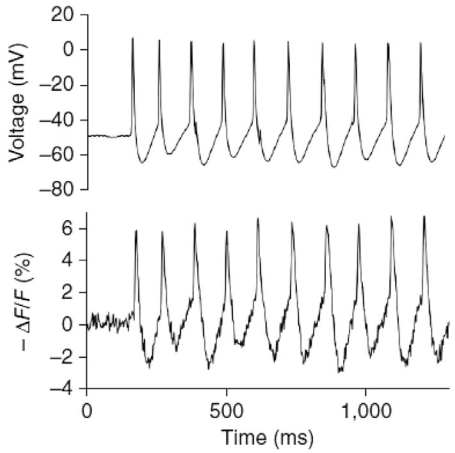

FIGURE 3 Imaging neural activity in current clamp-dissociated hippocampal cultures. ASAP1 followed a spontaneous AP train in a cultured hippocampal neuron ($\Delta F/F = -6.2 \pm 0.5\%$ mean $\pm$ SE, $n = 10$ APs). ASAP1 follows the membrane potential changes with high fidelity. Modified from (22).

Two-photon imaging. Chamberland et al. (50) have compared the signals from five recently developed GEVIs in detecting fast responses using two-photon imaging from single L2 cells in the *Drosophila* visual system. There was no detectable response to a visual stimulus using MacQ-mCitrine. With Ace-2N-2AA-mNeon there was a 1% signal. ASAP1, ASAP2s, and ArcLight had 5% signals. However, the response of both ASAP1 and ASAP2s declined to the baseline before the end of the visual stimulus in *Drosophila* and declined during the action potential in cardiomyocytes. Brinks et al. (51) measured two-photon lifetimes as a probe of absolute membrane voltage.

Mechanisms

There are different types of GEVIs with unique mechanisms that convert changes in membrane potential into optical signals (Fig. 1). Rhodopsin-based probes have a chromophore in the plasma membrane that responds to changes in the voltage field rapidly, compared to other types of GEVIs (Fig. 1 *B*, *type 2*). Thus far, these chromophores have very low quantum efficiencies requiring high intensity illumination for imaging (24,52,53). There have been no reports of the use of this kind of probe in mammalian central nervous system in vivo imaging, presumably because of the damage that such high intensities would cause. Addition of a cytoplasmic fluorescent protein improved the quantum efficiency and provides an optical signal via FRET quenching between the opsin chromophore and the fluorescent protein (25,54,55). Voltage-sensing domains from voltage-gated channels and the voltage-sensing phosphatase have also been used in the development of mosaic GEVIs (Fig. 1 *A*) (16,19,20,22,56,57). These GEVIs have the fluorescent chromophore outside of the voltage field. This usually resulted in slower probes ($\tau \sim 10$ ms) with the important exceptions of ElectricPk (58), ASAP1 (22), and Flicker (a red-shifted GEVI) (48).

In addition to differing voltage-sensitive domains, GEVIs also use different fluorescent protein designs. FRET pairs can exist as tandem fluorescent proteins at the carboxy-terminus (19,57,59,60) or flanking the voltage-sensitive domain (Fig. 1 *A*, *butterfly pair*) (21,61). Conformational changes of the voltage-sensitive domain in response to altered voltages causes a change in the distance and/or the orientation of the FRET chromophores, resulting in an optical signal. Voltage-sensitive domains can also be fused to a single fluorescent protein (Fig. 1 *A*, *single FP*) (20,41,62–64) or a circularly permuted form of the fluorescent protein (Fig. 1 *A*, *circularly permuted*) (22,48,58,65). Conformational changes of the voltage-sensitive domain alter the strain in the β-can structure of the cpFP, resulting in an optical signal. GEVIs with a single FP usually give small signals of 1–2% $\Delta F/F$/100 mV unless there is a negative charge on the outside

of the β-can structure of a pH-sensitive FP. The A227D mutation of superecliptic pHluorin increased the size of the signal to >40% $\Delta F/F$/100 mV in ArcLight (20,66).

A striking discovery. The mechanism that converts membrane potential changes into optical signals was not obvious for GEVIs that fuse a single FP onto a voltage-sensitive domain (Fig. 1 *A*, *single FP*), but, remarkably, dimerization (63) of environmentally sensitive FPs (67) seems to be important. Reducing the affinity for dimerization of the FP resulted in a substantial loss of the voltage-dependent optical signal (Fig. 4). Three mutations to the fluorescent protein (A206K, L221K, and F223R) disrupted the dimerization of the FP (68). The discovery of ArcLight involved an A227D mutation, which may have resulted in altered affinity for dimerization. Introduction of the other two monomeric-favoring mutations (L221K and F223R) resulted in very small voltage-dependent signals. These results suggested that the conformational changes in the voltage-sensitive domain move the FPs in relation to each other, thereby altering their environment and resulting in an optical signal. A schematic model of a dimer structure is illustrated in Fig. 4 *B*.

Important spectral properties of mosaic GEVIs have not been measured. These include detailed absorption and emission spectra, determining whether the signal arises from a change in absorption cross section or a change in emission quantum efficiency, and fluorescence lifetime measurements.

Larger and faster

Multiple characteristics of a GEVI contribute to the optical signal. The size of the signal depends in part on the voltage sensitivity, the range of voltages over which the sensor responds, and the speed of the probe. Probes with a sigmoidal fluorescence-voltage relationship have a maximum optical sensitivity at the voltage where the signal is 50% of maximum. The speed of the probe determines the percentage of the maximum optical signal that will be obtained for brief voltage changes. For instance, a probe that exhibits a 10% signal when the membrane potential changes from −70 to +30 mV with a τ of 2 ms would yield a roughly 6% signal for an action potential. Modifying the optical response for specific voltage ranges would improve the selectivity of population signals for action potentials or for subthreshold activities.

There are three relatively separate regions—the voltage-sensitive domain, the FP, and the linker between the two regions—and these regions have been modified to improve the optical signal. Mutations to the voltage-sensitive domain can improve the signal size and speed, and adjust the voltage sensitivity of type 1 (Fig. 1) GEVIs (19,41). Mutations to the FP can increase the signal size and alter the speed of the signal (20). Mutations to the FP can even invert the polarity of the optical signal causing the probe to get brighter instead of dimmer during depolarization of the plasma membrane (64). Using brighter FPs for electrochromic FRET improved the signal-to-noise ratio (25). Mutations to the linker region between the voltage-sensing domain and the FP also can improve the size of the signal and change the voltage-range of the probe (42,49). Altering the linker length of the Ace-mNeon family was used to optimize the plasma membrane expression in in vivo and in vitro preparations (25).

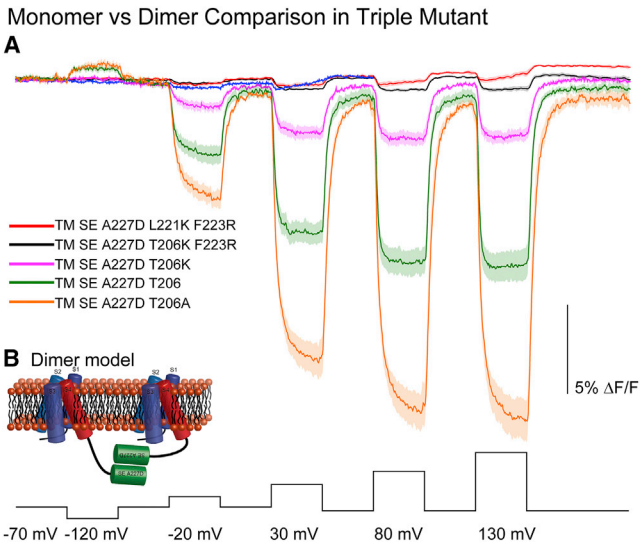

FIGURE 4 The Effect of monomeric mutations at the dimerization site of a single FP mosaic GEVI. (*A*) The GEVI triple mutant with 206A-221L-223F that favors dimerization has the largest signal (*orange*). Individual mutations favoring the monomer at the three sites reduced the signal (*green* and *purple*); double mutations cause a further reduction (*red* and *black*). (*B*) Given here is a schematic model of a triple mutant dimer. Modified from (54).

An internal signal

One advantage of imaging activity is that one can get information from regions that are not easily accessible to microelectrodes. Recently, in an attempt to alter the voltage sensitivity of a GEVI, mutations were introduced near the transition of transmembrane segment's α−helixes and the random coil structures of the loops connecting them. Nearly 40% of cells expressing these modified GEVIs show a high degree of internal expression as well as substantial plasma membrane expression. This is not unusual as misfolded protein is often retained in the endoplasmic reticulum. What was unusual was that these cells exhibited an internal optical signal in response to whole cell voltage-clamp steps. The signal was of opposite polarity from that seen in the plasma membrane of the same cell. Although these results are preliminary, they raise the exciting possibility that internal membranes can sense the voltage changes in the plasma membrane (M.S.R., L.B.C., O.B., and B.J.B., unpublished data).

Future perspectives

Efforts are presently underway along several directions to increase the utility of GEVIs.

Larger signal-to-noise ratios. These can come from several kinds of GEVI improvements: 1) larger and/or faster movements of the voltage-sensitive domain, 2) better coupling of the fluorescent protein to the voltage-sensitive domain, 3) increased brightness of the fluorescent protein (although some of the fluorescent proteins already in use have high quantum efficiencies), and 4) maximizing the monomer-dimer interaction in single FP mosaics.

Red-shifted GEVIs. These are important to allow measurements from more than one cell type or a measurement and an opto-genetic activation in the same brain region. Many of the presently available GEVIs are based on GFP fluorescent proteins and thus measurements from two cell types are not possible. There are new (and interesting) red GEVIs but their signal size is smaller than presently available green sensors (48).

Action potential or inhibition-only GEVIs useful in population measurements. Many mosaic (Fig. 1 *A*) GEVIs have nonlinear (sigmoidal) signal versus voltage relationships. Furthermore, the range of their voltage responses can be adjusted along the voltage axis (41) and thus they can be selectively sensitive to the membrane potential ranges that occur during action potentials or during inhibition. Furthermore, there is preliminary evidence that the steepness of the signal versus voltage relationship can be modified by inhibiting the movement of S4 in one direction (69) or by altering the charge in the linker region between the voltage-sensing domain and the FP (B. J. Yi, S. Braubach, and B. J. Baker, unpublished data).

Targeting the GEVI to defined subcellular domains. Presently available GEVIs express everywhere in the neuron. This is unattractive in many circumstances. If the object is to record activity from the cell body, then the signals from processes degrades the signal-to-noise ratio. If the object is to record from the nerve terminal, then the signal from the axon interferes. If the object is to record the activity from the mitral cell dendritic tufts in an olfactory cell glomerulus, then the expression in the lateral dendrites interferes. Clearly, the neuron knows how to target specific proteins to specific subcellular domains. We hope that the same subcellular targeting specificity can be developed for GEVIs.

Increased optical efficiency. There have been improvements in one- and two-photon optics that increased the recording speed or field of view (e.g., Sofroniew et al. (70)), but we are not aware of ideas for improving the optics in a way that will increase the fundamental signal-to-noise ratio of the sensor response.

ACKNOWLEDGMENTS

This work was supported by National Institutes of Health (NIH) grants DC005259, NS054270, NS099691, and DC016133; the Korea Institute of Science and Technology (KIST) grants 2E26190 and 2E26170; a James Hudson Brown-Alexander Brown Coxe fellowship from Yale University; and a Ruth L. Kirschstein National Research Service Award DC012981.

REFERENCES

1. Sherrington, S. C. 1937. Man on His Nature.. Cambridge University Press, Cambridge, UK.
2. St-Pierre, F., M. Chavarha, and M. Z. Lin. 2015. Designs and sensing mechanisms of genetically encoded fluorescent voltage indicators. *Curr. Opin. Chem. Biol.* 27:31–38.
3. Storace, D., M. S. Rad, …, U. Sung. 2015. Genetically encoded protein sensors of membrane potential. *Adv. Exp. Med. Biol.* 859:493–509.
4. Knöpfel, T., Y. Gallero-Salas, and C. Song. 2015. Genetically encoded voltage indicators for large scale cortical imaging come of age. *Curr. Opin. Chem. Biol.* 27:75–83.
5. Cohen, L. B., and B. M. Salzberg. 1978. Optical measurement of membrane potential. *Rev. Physiol. Biochem. Pharmacol.* 83:35–88.
6. Podgorski, K., and G. Ranganathan. 2016. Brain heating induced by near-infrared lasers during multiphoton microscopy. *J. Neurophysiol.* 116:1012–1023.
7. Wachowiak, M., and L. B. Cohen. 2001. Representation of odorants by receptor neuron input to the mouse olfactory bulb. *Neuron.* 32:723–735.
8. Bozza, T., A. Vassalli, …, P. Mombaerts. 2009. Mapping of class I and class II odorant receptors to glomerular domains by two distinct types of olfactory sensory neurons in the mouse. *Neuron.* 61:220–233.
9. Storace, D. A., and L. B. Cohen. 2017. Measuring the olfactory bulb input-output transformation reveals a contribution to the perception of odorant concentration invariance. *Nat. Commun.* 8:81.
10. McGann, J. P., N. Pírez, …, M. Wachowiak. 2005. Odorant representations are modulated by intra- but not interglomerular presynaptic inhibition of olfactory sensory neurons. *Neuron.* 48:1039–1053.
11. Davila, H. V., B. M. Salzberg, …, A. S. Waggoner. 1973. A large change in axon fluorescence that provides a promising method for measuring membrane potential. *Nat. New Biol.* 241:159–160.
12. Conti, F., and I. Tasaki. 1970. Changes in extrinsic fluorescence in squid axons during voltage-clamp. *Science.* 169:1322–1324.
13. Brown, J. E., L. B. Cohen, …, B. M. Salzberg. 1975. Rapid changes in intracellular free calcium concentration. Detection by metallochromic indicator dyes in squid giant axon. *Biophys. J.* 15:1155–1160.
14. Popovic, M. A., X. Gao, …, D. Zecevic. 2014. Cortical dendritic spine heads are not electrically isolated by the spine neck from membrane potential signals in parent dendrites. *Cereb. Cortex.* 24:385–395.
15. Popovic, M. A., N. Carnevale, …, D. Zecevic. 2015. Electrical behaviour of dendritic spines as revealed by voltage imaging. *Nat. Commun.* 6:8436.
16. Siegel, M. S., and E. Y. Isacoff. 1997. A genetically encoded optical probe of membrane voltage. *Neuron.* 19:735–741.
17. Guerrero, G., M. S. Siegel, …, E. Y. Isacoff. 2002. Tuning flaSh: redesign of the dynamics, voltage range, and color of the genetically encoded optical sensor of membrane potential. *Biophys. J.* 83:3607–3618.
18. Baker, B. J., H. Lee, …, E. K. Kosmidis. 2007. Three fluorescent protein voltage sensors exhibit low plasma membrane expression in mammalian cells. *J. Neurosci. Methods.* 161:32–38.
19. Dimitrov, D., Y. He, …, T. Knöpfel. 2007. Engineering and characterization of an enhanced fluorescent protein voltage sensor. *PLoS One.* 2:e440.
20. Jin, L., Z. Han, …, V. A. Pieribone. 2012. Single action potentials and subthreshold electrical events imaged in neurons with a fluorescent protein voltage probe. *Neuron.* 75:779–785.
21. Akemann, W., H. Mutoh, …, T. Knöpfel. 2012. Imaging neural circuit dynamics with a voltage-sensitive fluorescent protein. *J. Neurophysiol.* 108:2323–2337.

22. St-Pierre, F., J. D. Marshall, …, M. Z. Lin. 2014. High-fidelity optical reporting of neuronal electrical activity with an ultrafast fluorescent voltage sensor. *Nat. Neurosci.* 17:884–889.

23. Junge, W., and H. T. Witt. 1968. On the ion transport system of photosynthesis—investigations on a molecular level. *Z. Naturforsch. B.* 23:244–254.

24. Kralj, J. M., A. D. Douglass, …, A. E. Cohen. 2011. Optical recording of action potentials in mammalian neurons using a microbial rhodopsin. *Nat. Methods.* 9:90–95.

25. Gong, Y., C. Huang, …, M. J. Schnitzer. 2015. High-speed recording of neural spikes in awake mice and flies with a fluorescent voltage sensor. *Science.* 350:1361–1366.

26. Wang, D., Z. Zhang, …, M. B. Jackson. 2010. Improved probes for hybrid voltage sensor imaging. *Biophys. J.* 99:2355–2365.

27. Stosiek, C., O. Garaschuk, …, A. Konnerth. 2003. In vivo two-photon calcium imaging of neuronal networks. *Proc. Natl. Acad. Sci. USA.* 100:7319–7324.

28. Charpak, S., J. Mertz, …, K. Delaney. 2001. Odor-evoked calcium signals in dendrites of rat mitral cells. *Proc. Natl. Acad. Sci. USA.* 98:1230–1234.

29. Helmchen, F., K. Svoboda, …, D. W. Tank. 1999. In vivo dendritic calcium dynamics in deep-layer cortical pyramidal neurons. *Nat. Neurosci.* 2:989–996.

30. Schiller, J., G. Major, …, Y. Schiller. 2000. NMDA spikes in basal dendrites of cortical pyramidal neurons. *Nature.* 404:285–289.

31. Ross, W. N. 2012. Understanding calcium waves and sparks in central neurons. *Nat. Rev. Neurosci.* 13:157–168.

32. Emptage, N., T. V. Bliss, and A. Fine. 1999. Single synaptic events evoke NMDA receptor-mediated release of calcium from internal stores in hippocampal dendritic spines. *Neuron.* 22:115–124.

33. Garaschuk, O., Y. Yaari, and A. Konnerth. 1997. Release and sequestration of calcium by ryanodine-sensitive stores in rat hippocampal neurones. *J. Physiol.* 502:13–30.

34. Pozzo Miller, L. D., J. J. Petrozzino, …, J. A. Connor. 1996. Ca^{2+} release from intracellular stores induced by afferent stimulation of CA3 pyramidal neurons in hippocampal slices. *J. Neurophysiol.* 76:554–562.

35. Rose, T., P. M. Goltstein, …, O. Griesbeck. 2014. Putting a finishing touch on GECIs. *Front. Mol. Neurosci.* 7:88.

36. Callaway, J. C., and W. N. Ross. 1995. Frequency-dependent propagation of sodium action potentials in dendrites of hippocampal CA1 pyramidal neurons. *J. Neurophysiol.* 74:1395–1403.

37. Markram, H., P. J. Helm, and B. Sakmann. 1995. Dendritic calcium transients evoked by single back-propagating action potentials in rat neocortical pyramidal neurons. *J. Physiol.* 485:1–20.

38. Svoboda, K., W. Denk, …, D. W. Tank. 1997. In vivo dendritic calcium dynamics in neocortical pyramidal neurons. *Nature.* 385:161–165.

39. Wachowiak, M., M. N. Economo, …, M. Rothermel. 2013. Optical dissection of odor information processing in vivo using GCaMPs expressed in specified cell types of the olfactory bulb. *J. Neurosci.* 33:5285–5300.

40. Storace, D. A., O. R. Braubach, …, U. Sung. 2015. Monitoring brain activity with protein voltage and calcium sensors. *Sci. Rep.* 5:10212.

41. Piao, H. H., D. Rajakumar, …, B. J. Baker. 2015. Combinatorial mutagenesis of the voltage-sensing domain enables the optical resolution of action potentials firing at 60 Hz by a genetically encoded fluorescent sensor of membrane potential. *J. Neurosci.* 35:372–385.

42. Jung, A., J. E. Garcia, …, B. J. Baker. 2015. Linker length and fusion site composition improve the optical signal of genetically encoded fluorescent voltage sensors. *Neurophotonics.* 2:021012.

43. Peron, S., T. W. Chen, and K. Svoboda. 2015. Comprehensive imaging of cortical networks. *Curr. Opin. Neurobiol.* 32:115–123.

44. Empson, R. M., C. Goulton, …, T. Knöpfel. 2015. Validation of optical voltage reporting by the genetically encoded voltage indicator VSFP-Butterfly from cortical layer 2/3 pyramidal neurons in mouse brain slices. *Physiol. Rep.* 3:e12468, Epub 2015 Jul 29.

45. Borden, P. Y., A. D. Ortiz, …, G. B. Stanley. 2017. Genetically expressed voltage sensor ArcLight for imaging large scale cortical activity in the anesthetized and awake mouse. *Neurophotonics.* 4:031212.

46. Tsutsui, H., Y. Jinno, …, Y. Okamura. 2013. Improved detection of electrical activity with a voltage probe based on a voltage-sensing phosphatase. *J. Physiol.* 591:4427–4437.

47. Carandini, M., D. Shimaoka, …, T. Knöpfel. 2015. Imaging the awake visual cortex with a genetically encoded voltage indicator. *J. Neurosci.* 35:53–63.

48. Abdelfattah, A. S., S. L. Farhi, …, R. E. Campbell. 2016. A bright and fast red fluorescent protein voltage indicator that reports neuronal activity in organotypic brain slices. *J. Neurosci.* 36:2458–2472.

49. Lee, S., T. Geiller, …, B. J. Baker. 2017. Improving a genetically encoded voltage indicator by modifying the cytoplasmic charge composition. *Scientific Rep.* 7:8286.

50. Chamberland, S., H. H. Yang, …, F. St-Pierre. 2017. Fast two-photon imaging of subcellular voltage dynamics in neuronal tissue with genetically encoded indicators. *eLife.* 6:e25690.

51. Brinks, D., A. J. Klein, and A. E. Cohen. 2015. Two-photon lifetime imaging of voltage indicating proteins as a probe of absolute membrane voltage. *Biophys. J.* 109:914–921.

52. Hochbaum, D. R., Y. Zhao, …, A. E. Cohen. 2014. All-optical electrophysiology in mammalian neurons using engineered microbial rhodopsins. *Nat. Methods.* 11:825–833.

53. Lou, S., Y. Adam, …, A. E. Cohen. 2016. Genetically targeted all-optical electrophysiology with a transgenic cre-dependent optopatch mouse. *J. Neurosci.* 36:11059–11073.

54. Zou, P., Y. Zhao, …, A. E. Cohen. 2014. Bright and fast multicoloured voltage reporters via electrochromic FRET. *Nat. Commun.* 5:4625.

55. Gong, Y., M. J. Wagner, …, M. J. Schnitzer. 2014. Imaging neural spiking in brain tissue using FRET-opsin protein voltage sensors. *Nat. Commun.* 5:3674.

56. Ataka, K., and V. A. Pieribone. 2002. A genetically targetable fluorescent probe of channel gating with rapid kinetics. *Biophys. J.* 82:509–516.

57. Sakai, R., V. Repunte-Canonigo, …, T. Knöpfel. 2001. Design and characterization of a DNA-encoded, voltage-sensitive fluorescent protein. *Eur. J. Neurosci.* 13:2314–2318.

58. Barnett, L., J. Platisa, …, T. Hughes. 2012. A fluorescent, genetically-encoded voltage probe capable of resolving action potentials. *PLoS One.* 7:e43454.

59. Baker, B. J., L. Jin, …, V. Pieribone. 2012. Genetically encoded fluorescent voltage sensors using the voltage-sensing domain of Nematostella and Danio phosphatases exhibit fast kinetics. *J. Neurosci. Methods.* 208:190–196.

60. Lundby, A., W. Akemann, and T. Knöpfel. 2010. Biophysical characterization of the fluorescent protein voltage probe VSFP2.3 based on the voltage-sensing domain of Ci-VSP. *Eur. Biophys. J.* 39:1625–1635.

61. Sung, U., M. Sepehri-Rad, …, B. J. Baker. 2015. Developing fast fluorescent protein voltage sensors by optimizing FRET interactions. *PLoS One.* 10:e0141585.

62. Lundby, A., H. Mutoh, …, T. Knöpfel. 2008. Engineering of a genetically encodable fluorescent voltage sensor exploiting fast Ci-VSP voltage-sensing movements. *PLoS One.* 3:e2514.

63. Kang, B. E., and B. J. Baker. 2016. Pado, a fluorescent protein with proton channel activity can optically monitor membrane potential, intracellular pH, and map gap junctions. *Sci. Rep.* 6:23865.

64. Platisa, J., G. Vasan, …, V. A. Pieribone. 2017. Directed evolution of key residues in fluorescent protein inverses the polarity of voltage sensitivity in the genetically encoded indicator ArcLight. *ACS Chem. Neurosci.* 8:513–523.

65. Perron, A., H. Mutoh, …, T. Knöpfel. 2009. Second and third generation voltage-sensitive fluorescent proteins for monitoring membrane potential. *Front. Mol. Neurosci.* 2:5.

66. Han, Z., L. Jin, …, V. A. Pieribone. 2013. Fluorescent protein voltage probes derived from ArcLight that respond to membrane voltage changes with fast kinetics. *PLoS One.* 8:e81295.

67. Han, Z., L. Jin, …, V. A. Pieribone. 2014. Mechanistic studies of the genetically encoded fluorescent protein voltage probe ArcLight. *PLoS One.* 9:e113873.

68. Zacharias, D. A., J. D. Violin, …, R. Y. Tsien. 2002. Partitioning of lipid-modified monomeric GFPs into membrane microdomains of live cells. *Science.* 296:913–916.

69. Jung, A., D. Rajakumar, …, B. J. Baker. 2017. Modulating the voltage-sensitivity of a genetically-encoded voltage indicator. *Exp. Neurobiol.* 5:241–251.

70. Sofroniew, N. J., D. Flickinger, …, K. Svoboda. 2016. A large field of view two-photon mesoscope with subcellular resolution for in vivo imaging. *eLife.* 5:e14472.